



University of Nebraska at Omaha  
DigitalCommons@UNO

---

Journal Articles

Department of Biomechanics

---

2010

# Complexity and Human Gait

Leslie M. Decker

*University of Nebraska at Omaha*

Fabien Cignetti

*University of Nebraska at Omaha*

Nicholas Stergiou

*University of Nebraska at Omaha, [nstergiou@unomaha.edu](mailto:nstergiou@unomaha.edu)*

Follow this and additional works at: <https://digitalcommons.unomaha.edu/biomechanicsarticles>

 Part of the [Biomechanics Commons](#)

---

## Recommended Citation

Decker, Leslie M.; Cignetti, Fabien; and Stergiou, Nicholas, "Complexity and Human Gait" (2010). *Journal Articles*. 91.  
<https://digitalcommons.unomaha.edu/biomechanicsarticles/91>

This Article is brought to you for free and open access by the Department of Biomechanics at DigitalCommons@UNO. It has been accepted for inclusion in Journal Articles by an authorized administrator of DigitalCommons@UNO. For more information, please contact [unodigitalcommons@unomaha.edu](mailto:unodigitalcommons@unomaha.edu).



1 **Complexity and Human Gait**

2

3 Leslie M. Decker<sup>1</sup>, Fabien Cignetti<sup>1</sup>, Nicholas Stergiou<sup>1,2,\*</sup>

4 <sup>1</sup>Nebraska Biomechanics Core Facility, University of Nebraska at Omaha, 6001 Dodge Street, Omaha, NE  
5 68182-0216, USA.

6 <sup>2</sup>Department of Environmental, Agricultural and Occupational Health Sciences, College of Public Health,  
7 University of Nebraska Medical Center, 987850 Nebraska Medical Center, Omaha, NE 68198-7850, USA.

8 \*Corresponding author. Nebraska Biomechanics Core Facility, University of Nebraska at Omaha, 6001  
9 Dodge Street, Omaha, NE 68182-0216, USA. Tel.: 402-5543247. Fax: 402-5543693. E-mail address:  
10 nstergiou@unomaha.edu

11 **Abstract**

12 Recently, the complexity of the human gait has become a topic of major interest within the field of human  
13 movement sciences. Indeed, while the complex fluctuations of the gait patterns were, for a long time,  
14 considered as resulting from random processes, the development of new techniques of analysis, so-called  
15 nonlinear techniques, has open new vistas for the understanding of such fluctuations. In particular, by  
16 connecting the notion of complexity to the one of chaos, new insights about gait adaptability, unhealthy  
17 states in gait and neural control of locomotion were provided. Through methods of evaluation of the  
18 complexity, experimental results obtained both with healthy and unhealthy subjects and theoretical models  
19 of gait complexity, this review discusses the tremendous progresses made about the understanding of the  
20 complexity in the human gait variability.

21

22

23 **Key-Words**

24 Gait, Variability, Complexity, Chaos, Aging, Diseases, Modeling, Neural Control.

## 25 1. Introduction

26 Despite the numerous operations involved during human gait (activation of the central nervous system,  
27 transmission of the signals to the muscles, contraction of the muscles, integration of the sensory  
28 information, etc.), the way in which humans move appears stable with quite smooth, regular and repeating  
29 movements<sup>1</sup>. Besides, investigations using biomechanical (i.e., kinematics, kinetic and electromyographic)  
30 measures seem to confirm this impression with patterns relatively constant across the gait cycles. However,  
31 closer and more careful examinations of the gait patterns highlighted complex fluctuations over time, the  
32 patterns never repeating exactly as themselves<sup>2-4</sup>. Until recently, these variations were considered as noisy  
33 variations, resulting from some random processes. However, recent literature from different scientific  
34 domains has shown that many phenomena previously described as noisy are actually the results of  
35 nonlinear interactions and have deterministic origins, conveying important information regarding the  
36 system behavior<sup>5-7</sup>.

37 Therefore, arrays of investigation have been conducted to characterize and understand the complex  
38 fluctuations observed in gait<sup>2-4,8-17</sup>. Using tools from nonlinear dynamics, these studies demonstrated that  
39 this complexity is responsible for the flexible adaptations to everyday stresses placed on the human body  
40 during gait. They also established a link between the alterations of this complexity and the unhealthy states  
41 in gait. Therefore, the aim of this review is to present, in the more exhaustive manner as possible in view of  
42 the space constraints, the progresses made recently about the understanding of the complexity in the  
43 human gait.

44 The first section of the review is dedicated to the definition and the function of complexity using well-  
45 known physiological rhythms. The second section is interested in normal gait, investigating its complexity  
46 through the most commonly used nonlinear parameters. In a third section the relationship between gait  
47 complexity and unhealthy states is presented. Then, in a last section some models of gait complexity, with  
48 an emphasis on the possible neural mechanisms responsible for this complexity, are presented.

## 49 2. What is complexity?

50 Like the beating of the heart, the cycles of the respiration or the impulses of the nerve cells, bodily  
51 rhythms are ubiquitous in humans and central to life<sup>6,18-20</sup>. Accordingly, they have been coming under  
52 increasingly closer examination. A common finding is that these rhythms are rarely strictly periodic, but  
53 rather complex, fluctuating in an irregular way over time (nice illustrations of complex human rhythms are  
54 available in Glass<sup>20</sup>). The most interesting fact is that these irregular fluctuations, initially viewed as the  
55 result of some stochastic (noisy) processes<sup>6</sup>, were recently found to have deterministic origins. Results  
56 obtained from experiments investigating beat-to-beat intervals of the human heart, the so-called R-R  
57 intervals, are perfect illustrations of such determinism. Anybody who listen the beats of the heart feels that  
58 the rhythm is regular with a roughly constant R-R interval between the beats. However, using techniques  
59 from nonlinear dynamics which will be detailed next, studies highlighted that the R-R intervals varied over  
60 time (Fig. 1), and more interesting, proved that the R-R interval at any time depends on the R-R interval at  
61 remote previous time<sup>21-26</sup>. The irregular fluctuations in the beating of the heart, which appear first to be

62 erratic, are then fully deterministic, this “constrained kind of randomness” meaning that the heart  
63 dynamics (i.e., its behavior over time) is chaotic. Hence, the concept of complexity for which we take  
64 major interest in the present work is profoundly connected with the one of chaos and can be defined, as  
65 proposed by Stergiou et al.<sup>27</sup>, as the irregular (variable) fluctuations that appear in physiological rhythms  
66 which take the form of chaos.

67 *Please insert Fig. 1 here*

68 Considering now that bodily rhythms are complex in the sense that they display chaotic fluctuations  
69 over time, an interesting question is the one of the function of complexity. Numerous studies suggested that  
70 the chaotic temporal variations represent capabilities to make flexible adaptations to everyday stresses  
71 placed on the human body<sup>21,25,28</sup>. A reduction or deterioration of the chaotic nature of these temporal  
72 variations represents a decline in the “healthy flexibility” that is associated with rigidity and inability to  
73 adapt to stresses<sup>21,25,28</sup>. Findings from experiments in cardiology illustrate again such phenomenon. While  
74 either random or periodic (i.e., constant) variations in the R-R interval of the heart beat are associated with  
75 disorders, chaotic heart rhythms are related to healthy states (e.g., Goldberger et al.<sup>28</sup>). Using the above  
76 idea as a foundation, Stergiou et al.<sup>27</sup> have proposed a model to explain the rhythms complexity as it  
77 relates to health. In this theoretical model, greater complexity is characterized by chaotic fluctuations and  
78 is associated with a healthy state of the underlying system while lesser amounts of complexity are  
79 associated with both periodic and random fluctuations where the system is either too rigid or too unstable  
80 (Fig. 2). Both situations characterize systems that are less adaptable to perturbations, such as those  
81 associated with unhealthy states. The notion of predictability has also been implemented in the model,  
82 mainly to differentiate between the random and periodic rhythms. Indeed, low predictability is associated  
83 with random and noisy systems, while high predictability is associated with periodic highly repeatable and  
84 rigid behaviours. In between is chaotic, highly complex, based-behaviours where the systems are neither  
85 too noisy nor too rigid (Fig. 2). Therefore, the complex fluctuations of the human rhythms are intrinsic and  
86 vital to the operation of the underlying systems, a deterioration of complexity being harmful to their  
87 operation.

88 *Please insert Fig. 2 here*

89 Directly related to the previous concerns is the human gait. Indeed, human gait is also rhythmic by  
90 nature, involving repeatable motions of the joints and successive step and stride cycles. Accordingly, does  
91 such a rhythmic activity also characterized by some complex (chaotic) fluctuations? And if the fluctuations  
92 are chaotic, is there some reasons to believe that their alteration reflect unhealthy states? Studies bring  
93 significant answers to these interrogations.

### 94 **3. Complexity of the human gait**

95 To investigate the complexity of the human gait, many investigations have examined whether the  
96 rhythms related to human walking, such as the linear or angular rhythmical motions of the joints and the  
97 stride-time interval, display chaotic fluctuations over time using two different kinds of analyses based on 1)  
98 state space examination and 2) self-similarity evaluation<sup>2-4,8-11,12-14</sup>.

#### 99 **3.1 State space examination**

100 The state space analysis represents a technique which consists in representing the dynamics of the joint  
 101 movements in an abstract, multi-dimensional space, where the coordinates represents simply the values of  
 102 some state variables characterizing the joint<sup>4,29-31</sup>. In such a space, the set of all possible states that can be  
 103 reached corresponds to the phase space. The sequence of such states over the time-scale defines a curve in  
 104 the phase space called a trajectory and as time increases, the trajectory converges towards a low-  
 105 dimensional indecomposable subset called an attractor which gives information about the asymptotic  
 106 behaviour (periodic, chaotic or random) of the joint<sup>4</sup>. However, since one cannot measure experimentally  
 107 all the components of the vector characterizing the state of the joints, the authors have reconstructed the  
 108 state space from one-dimensional joint kinematics data sets, by using the time delay method derived from  
 109 the Takens' embedding theorem<sup>32,33</sup>. Specifically, different scalar kinematics measures were used to  
 110 reconstruct state space including joint angles<sup>4,34</sup>, linear joints displacements or accelerations<sup>12,14,35-37</sup> and  
 111 Euler angles at the joints<sup>38</sup>. Hence, given a time series (Fig. 3A)

$$112 \quad \{x_i\}_{i=1}^N \quad (1)$$

113 of  $N$  kinematics joint data sampled at equal time intervals, the reconstructed attractor consists of a set of  $m$ -  
 114 dimensional vectors  $v_i, i = 1, \dots, N - (m-1)\tau$  of the form

$$115 \quad v_i = (x_i, x_{i+\tau}, x_{i+2\tau}, \dots, x_{i+(m-1)\tau}) \quad (2)$$

116 where  $\tau$  is the time delay, chosen to maximize the information content of  $x_i$ , and  $m$  the embedding  
 117 dimension that must be large enough to “unfold” the attractor (Fig. 3B). Choice of the delay was generally  
 118 accomplished by looking for the first minimum of the average mutual information function<sup>39</sup> whereas the  
 119 embedding dimension was selected where the percentage of the global false nearest neighbours approached  
 120 zero<sup>40</sup>. Despite variations in the kinematics parameters used to reconstruct the state space as mentioned  
 121 above, all highlighted appropriate embedding dimensions higher than two (most of time around five),  
 122 indicating that the attractors underlying the joints movements during human walking exceed a periodic  
 123 attractor, converging possibly towards a strange attractor and suggesting that the observed movement's  
 124 patterns fluctuate over time in a chaotic way<sup>3,12-14</sup>.

125 Moreover, different index looking at the structure of the attractors were also calculated to strengthen  
 126 the presence of chaos in gait, including the largest Lyapunov exponent ( $\lambda_1$ ) and the correlation dimension  
 127 ( $D_c$ ), the former measuring the average exponential rate of divergence of neighbouring trajectories of the  
 128 attractor<sup>29,41</sup> and the latter the way in which the attractor's geometry varies over many orders of the  
 129 attractor's length scales<sup>42,43</sup>. Technically,  $\lambda_1$  is calculated in gait using the algorithm developed by  
 130 [Rosenstein et al.](#)<sup>41</sup>, which applies well to time series of finite length, following:

$$131 \quad \ln d_j(i) \approx \lambda_1(i, \Delta t) + \ln D_j, \quad (3)$$

132 where  $\Delta t$  is the sampling period of the time series and  $d_j(i)$  is the Euclidean distance between the  $j^{\text{th}}$  pair  
 133 of nearest neighbours after  $i$  discrete-time steps, i.e.,  $i, \Delta t$  s. Euclidean distances between neighbouring  
 134 trajectories are calculated as a function of time and averaged over all original pairs of nearest neighbours.  
 135 The  $\lambda_1$  is then estimated from the slope of the linear fit to curve defined by:

136  $y(i) = \frac{1}{\Delta t} \langle \ln d_j(i) \rangle,$  (4)

137 where  $\langle \cdot \rangle$  denotes the average over all values of  $j$  (Fig. 3C). On the other hand, the correlation dimension  
 138 is estimated by measuring how the average number of points within an (hyper) sphere of radius  $r$  centred  
 139 on the attractor scales with  $r$ , based on the calculation of the correlation integral<sup>44</sup>:

140 
$$C(r) = \frac{1}{N^2} \sum_{\substack{i,j=1 \\ i \neq j}}^N \theta(r - |v_i - v_j|),$$
 (5)

141 where  $\theta(\cdot)$  is the Heaviside function, i.e.,  $\theta(r - |v_i - v_j|) = \begin{cases} 1 : r - |v_i - v_j| \geq 0 \\ 0 : r - |v_i - v_j| < 0 \end{cases}$ , and  $v_i, v_j$  are the vectors

142 previously defined in Eq.(2). For small values of  $r$ , the correlation integral behaves as a power of  $r$ , so that  
 143  $C(r) \propto r^{D_c}$ . Hence:

144 
$$C(r) \propto \lim_{r \rightarrow 0} r^{D_c} \quad \text{or} \quad D_c \propto \lim_{r \rightarrow 0} \frac{\ln C(r)}{\ln r}$$
 (6) and (7)

145 and  $D_c$  is then obtained by extracting the slope of the  $\ln/\ln$  plots of  $C(r)$  vs.  $r$  (Fig. 3D). In line with the  
 146 results from the embedding dimensions, the  $\lambda_l$  and  $D_c$  values picked out through the literature are  
 147 systematically positive and higher than one<sup>3,12,14,35,36</sup>, reinforcing the idea that a “low-deterministic” chaos  
 148 is present in the gait data.

149 *Please insert Fig. 3 here*

150 However, even though previous results strongly favour a chaotic nature of the fluctuations present in  
 151 the gait patterns, all are hindered by the fact that the identification of chaos in time series is a very difficult  
 152 process since purely random signals can mimic chaos and have sometimes been misdiagnosed as chaotic or  
 153 vice versa<sup>45,46</sup>. Thus, methods known as surrogate analyses have been used in gait to prevent such  
 154 misdiagnoses<sup>3,4,14,47</sup>. Technically, these analyses consist in the creation of a random counterpart of the  
 155 original data, by destroying its nonlinear structure. This counterpart is then embedded in an equivalent  
 156 state space as the one of the original time series and similar topological parameters as those obtained from  
 157 the original time series are calculated (e.g.,  $\lambda_1$  and  $D_c$ ). Accordingly, differences in the parameters  
 158 evaluated from the original data set and its surrogate counterpart indicate that the fluctuations over time in  
 159 the original data are veritably chaotic and not randomly derived. The surrogate algorithms of Theiler et  
 160 al.<sup>46</sup> and Theiler and Rapp<sup>48</sup> has been used in the past and related results support the notion that  
 161 fluctuations in human gait have a deterministic pattern<sup>2,3,14</sup>. However, these algorithms have been shown  
 162 of limited utility when applied to time series with strong pseudo-periodic behaviours as it is the case in gait  
 163 (see Fig. 3A and 3B). Thus, Small et al.<sup>49</sup> have consequently proposed another algorithm, the so-called  
 164 pseudo-periodic surrogate (PPS) algorithm, to preserve such periodicities (i.e., to preserve intra-cycle  
 165 dynamics while destroying inter-cycle dynamics). In a recent work conducted on gait data, Miller et al.<sup>47</sup>  
 166 showed that both algorithms attest for the presence of chaotic fluctuations in gait, with more robust and  
 167 suitable results using the PPS algorithm. Hence, using methods related to state space examination, the

168 fluctuations in the gait patterns have been found to be chaotic, demonstrating the complexity of the human  
 169 gait.

### 170 3.2 Self-similarity evaluation

171 The complexity of the human gait has also been evaluated using methods that evaluate the self-  
 172 similarity of the time series, by examining the presence of repetitive patterns in their fluctuations over time.  
 173 Among these methods, two have been extensively used in the gait literature: the Approximate Entropy and  
 174 the Detrended Fluctuation Analysis. The Approximate Entropy (*ApEn*) is strictly speaking a “regularity  
 175 statistic” that quantifies the unpredictability of fluctuations in a time series and reflects the probability that  
 176 similar patterns of observations will not be followed by additional similar observations<sup>50,51</sup>. This means that  
 177 a time series containing many repetitive patterns has a relatively small *ApEn* value, while a less predictable  
 178 (i.e., more complex) time series has a higher *ApEn* value. In human gait, computation of the *ApEn* has been  
 179 done from kinematics data including joint angle time series<sup>4,47,52</sup> and step count values<sup>53</sup>. Specifically, the  
 180 computation of *ApEn*, better identified as *ApEn(N,r,m)*, requires a time series consisting of *N* kinematics  
 181 data (as the one defined in equation 1) and two additional input parameters, *m* and *r*, the former specifying  
 182 the pattern length window and the latter a criterion of similarity. Note that a value of two data points for *m*  
 183 and a value of 0.2 times the time series standard deviation for *r* were used in gait studies. Hence, a vector  
 184  $p_m(i)$  is denoted as a subsequence (or pattern) of *m* kinematics data, beginning at measurement *i* within  
 185 the *N* input data points. Two patterns,  $p_m(i)$  and  $p_m(j)$ , are similar if the difference between any pair of  
 186 corresponding measurements in the patterns is less than *r*. Considering now the set  $P_m$  of all patterns of  
 187 length *m* [i.e.,  $p_m(1), p_m(2), \dots, p_m(N - m + 1)$ ] within the *N* data points, it is possible to define

$$188 \quad C_{im}(r) = \frac{n_{im}(r)}{N - m + 1} \quad (8)$$

189 where  $n_{im}(r)$  is the number of patterns in  $P_m$  that are similar to  $p_m(i)$ . The quantity  $C_{im}(r)$  corresponds  
 190 to the fraction of patterns of length *m* that resemble the pattern of the same length that begins at interval *i*.  
 191  $C_{im(r)}$  is then calculated for each pattern in  $P_m$  and the quantity  $C_m(r)$  is defined as the mean of these  
 192  $C_{im}(r)$  values. The quantity  $C_m(r)$  expresses then the prevalence of repetitive patterns of length *m* in the  
 193 *N* data points. Finally, the approximate entropy of the *N* data points, for patterns of length *m* and similarity  
 194 criterion *r*, is defined as the natural logarithm of the relative prevalence of repetitive patterns of length *m*  
 195 compared with those of length *m+1* as follows:

$$196 \quad ApEn(N, m, r) = \ln \left[ \frac{C_m(r)}{C_{m+1}(r)} \right] \quad (9)$$

197 In gait, the *ApEn* values obtained from joint kinematics and step count values were found generally in the  
 198 range [0.1-0.2]<sup>4,47,52,53</sup>, which corresponds to small values given the fact that the *ApEn* algorithm generates  
 199 numbers ranged from 0 (periodic data) to 2 (random data)<sup>50</sup>. Accordingly, the probability that similar  
 200 patterns are followed by additional similar patterns in the gait time series is high, reflecting a high level of



201 predictability. Despite such results would seem to prove that chaotic fluctuations are present in the gait  
 202 patterns, an important point which needs to be mentioned here is that  $ApEn$  is not genuinely able to  
 203 dissociate between chaotic and random fluctuations of the gait patterns. To counter such a limitation,  
 204 [Miller et al.](#)<sup>47</sup> have also applied surrogation techniques to their  $ApEn$  calculations and obtained  $ApEn$   
 205 values from the surrogated gait data (both Theiler and PPS algorithms) larger than the original  $ApEn$  values,  
 206 concluding on the presence of subtle chaotic fluctuations that appear in gait.

207 The Detrended Fluctuations Analysis (*DFA*) represents a modification of classic root mean square  
 208 analysis of random walk and evaluates the presence of long-term correlations within the time series, which  
 209 correspond to a statistical dependence between fluctuations at one time scale and those over multiple time  
 210 scales<sup>2,54</sup>. In human gait, the authors have considered time series of stride-time interval<sup>2,8,9,55</sup> and step  
 211 width<sup>56</sup>. Methodologically, the series  $x(t)$  of  $N$  data points is first integrated by computing for each  $t$  the  
 212 accumulated departure from the mean of the whole series:

$$213 \quad X(i) = \sum_{t=1}^i [x(t) - \bar{x}] \quad (10)$$

214 This integrated series is divided into non-overlapping intervals of length  $n$ . In each interval, a least squares  
 215 line is fit to the data (representing the trend in the interval) (Fig. 4A and 4B). The series  $X(t)$  is then locally  
 216 detrended by subtracting the theoretical values  $X_{th}(t)$  given by the regression. For a given interval length  $n$ ,  
 217 the characteristic size of fluctuation for this integrated and detrended series is calculated by:

$$218 \quad F(n) = \sqrt{\frac{1}{N} \sum_{k=1}^N [X(k) - X_{th}(k)]^2} \quad (11)$$

219 This computation is repeated over all possible interval lengths (in practice, the shortest length is around 10  
 220 data points, and the largest  $N/2$ , giving two adjacent intervals). Typically,  $F(n)$  increases with interval  
 221 length  $n$ . A power law is expected, as

$$222 \quad F(n) \propto n^\alpha \quad (12)$$

223 where  $\alpha$  is the scaling exponent, or self-similarity parameter.  $\alpha$  is then expressed as the slope of a double  
 224 logarithmic plot of  $F(n)$  as a function of  $n$  (Fig. 4C), and can vary between 0 and 1.5. Especially, when  $\alpha$  is  
 225 0.5, the original series was generated by an independent random process (white noise) and if  $\alpha$  is higher  
 226 than 0.5 and lower than or equal to 1, the series is characterized by long-term correlations and self-  
 227 similarity. Looking at the stride-time interval, [Hausdorff et al.](#)<sup>2</sup> observed  $\alpha$  values around 0.75 indicating  
 228 that fluctuations in the interval are, on average, related to variations in the interval hundreds of strides  
 229 earlier in a scale-invariant manner, so-called fractal manner. These long-term correlations in the stride-time  
 230 interval were found again in another work looking at subjects who walk for one hour at preferred, slow and  
 231 fast paces with an averaged  $\alpha$  value of 0.95<sup>8</sup>. Subsequent studies reiterated these findings in normal walking  
 232 and running investigating the stride-time interval<sup>57-59</sup> or new input data as time series of step width<sup>56</sup>. The  
 233 fluctuations of the stride interval and the step width in human gait are then structured rather than random  
 234 over time. This “long-memory process”, with each value depending upon the global history of the series,  
 235 reinforces again the chaotic character of the human gait.

236 *Please insert Fig. 4 here*

237 In sum, all the studies using state space examination and self-similarity evaluation tools stress the fact  
238 that normal human gait is intrinsically chaotic and according to our definition of complexity is highly  
239 complex, providing flexibility to adapt to perturbations that occur during displacement. The next section  
240 will examine how such complexity in human gait evolves with health- and disease-related aging.

#### 241 4. Relationship between gait complexity and health- and disease-related aging

##### 242 4.1. State space examination

243 Several researchers evaluated the effect of aging on gait complexity. A striking example of such studies  
244 is the one by [Buzzi et al.<sup>14</sup>](#), in which the authors investigated the nature (organization) of gait variability  
245 present in elderly and young women. Based on the assumption that aging may lead to changes in motor  
246 variability, the authors used nonlinear state space examination tools (largest Lyaunov exponent  $\lambda_1$  and  
247 correlation dimension  $D_C$ ) to compare kinematic variables between the two age groups. Thirty gait cycles  
248 (i.e., 8-min data collection) were recorded, allowing the examination of an average of 2441 data points for  
249 each variable. The selected kinematic variables were the hip, knee, and ankle  $y$ -coordinates (vertical  
250 displacement) and the relative knee angles. The elderly exhibited significantly larger  $\lambda_1$  values (hip: 0.22 vs.  
251 0.18, knee: 0.14 vs. 13, ankle: 0.10 vs. 0.08, knee angles: 0.15 vs. 0.11) and  $D_C$  values (hip: 3.44 vs. 3.02,  
252 knee: 3.54 vs. 2.94, ankle: 3.35 vs. 2.89, knee angles: 2.63 vs. 2.35) than the young for all parameters  
253 evaluated indicating more divergence in the movement trajectories along with more degrees of freedom at  
254 each joint. An additional observation from the results is that the  $\lambda_1$  increased from the ankle toward the hip,  
255 which can be due to the ground restriction at the lower end and thus, decrease in the available degrees of  
256 freedom. The knee and particularly the hip are also associated with a greater amount of musculature, thus  
257 producing an increasing variety of movements (i.e., increased degrees of freedom available at these joints).  
258 The authors hypothesized that the elderly exhibit more noise (i.e., less complexity as described in our  
259 model) in their gait patterns, likely explaining the higher incidence of falls in the elderly.

260 Other researchers seek to understand how individuals compensate for a disease. For instance, [Dingwell](#)  
261 [et al.<sup>12</sup>](#) investigated the effect of diabetic neuropathy on the lower extremity joint angles and the triaxial  
262 accelerations of the trunk collected during a 10-min walk at self-selected pace. The results showed that  
263 neuropathic patients exhibited smaller  $\lambda_1$  values in comparison with matched healthy controls (mean  $\lambda_1$ :  
264  $\sim 0.03$  vs.  $\sim 0.04$ , respectively). These patients also exhibited slower walking velocities (mean velocity: 1.24  
265  $\text{m}\cdot\text{s}^{-1}$  vs. 1.47  $\text{m}\cdot\text{s}^{-1}$ , respectively). This latter finding was explained as a compensatory strategy to maintain  
266 dynamic balance. More recently, [Myers et al.<sup>60</sup>](#) investigated the limitations caused by peripheral arterial  
267 disease, a chronic obstructive disease of the arteries of the lower limb caused by atherosclerosis. The  
268 resultant decrease in blood flow can result in symptoms of pain in the lower limb on exercise known as  
269 intermittent claudication. Exercise induced pain is experienced in the calves, thigh or buttocks restricting  
270 activities of daily living and thus reducing quality of life. These limitations are more pronounced in older  
271 patients, making them more prone to falls, possible need for nursing home placement and subsequent loss  
272 of functional independence. In this study, the authors examined whether the largest Lyapunov exponent, a  
273 measure of the sensitive dependence on the initial conditions, has clinical potential as a tool for early  
274 detection and/or prediction of the onset of peripheral arterial disease (PAD). For this purpose, joint angle  
275 variability of the lower extremities was evaluated in claudicating patients as compared with matched

276 controls during treadmill walking. Participants walked for three minutes or until the onset of claudication,  
277 whichever came first. Each joint angle time series included at least 30 strides before the onset of  
278 claudication. PAD patients had significantly higher  $\lambda_1$  for all joints compared with controls (hip: 0.095 vs.  
279 0.078, knee: 0.098 vs. 0.074, ankle: 0.105 vs. 0.078, respectively), indicating increased randomness in their  
280 gait patterns and loss of motor control. Interestingly, these differences in  $\lambda_1$  values were observed in the  
281 pain free condition, meaning that pain itself was not the source of increased divergence in the lower  
282 extremity movement trajectories. Most likely, the altered kinematic strategy for the control of gait reflects a  
283 combination of myopathy and neuropathy. The nature of these myopathic and neuropathic changes and  
284 the way they are associated with the clinical and biomechanical findings of leg dysfunction may hold the  
285 key to understanding the PAD pathophysiology.

## 286 4.2. Self-similarity evaluation

### 287 4.2.1. Approximate entropy

288 [Kurz and Stergiou<sup>61</sup>](#) used the statistical concept of entropy to explore the certainty present in the lower  
289 extremity joint kinematics during gait. Specifically, their study addresses the question of whether the  
290 neurophysiological changes associated with aging hinder the ability of the nervous system to appropriately  
291 select neural pathways for a stable and functional gait. The results supported the authors' hypothesis that  
292 aging is associated with less certainty in the neuromuscular system for selecting joint kinematics during gait.  
293 They speculated that less certainty may be due to neurophysiological changes associated with aging. Such  
294 neurophysiological changes can result in inaccurate information from the visual, vestibular, and  
295 somatosensory receptors (proprioceptive, cutaneous, and joint receptors). Thus, the aging neuromuscular  
296 system may not receive appropriate information to be certain that the selected kinematic behavior will  
297 provide a stable gait. Such uncertainty may be responsible for the increased probability of falls in the  
298 elderly.

299 Later, [Khandoker et al.<sup>62</sup>](#) applied ApEn for variability analysis of minimum foot clearance (MFC) data  
300 obtained from healthy elderly and falls-risk elderly (i.e., with balance problems and a history of falls).  
301 Minimum foot clearance, which occurs during the mid-swing phase of the gait cycle, has been identified as  
302 a sensitive gait variable for detecting change in the gait. In fact, at the MFC event, the foot travels very  
303 close to the walking surface (i.e., mean MFC height is approximately 1.29 cm) and even closer as  
304 individuals age (~ 1.12 cm). A decreased mean MFC height combined with its variability provides a strong  
305 rationale for MFC being associated with the risk of tripping and/or losing balance. Participants completed  
306 about 10 to 20 minutes of self-paced walking. For each participant, a dataset of 400 adjacent MFC points  
307 was used. Each dataset was divided into smaller sets of length ( $m = 2$ ), thus creating 200 smaller subsets.  
308 Then, the number of subsets that are within the criterion of similarity (i.e., 0.15 of the standard deviation of  
309 400 MFC points) was determined. The same process was repeated for the second subset till each subset was  
310 compared with the rest of the dataset. The results reveal that ApEn, used with  $m = 3$ , in falls-risk elderly  
311 (i.e., mean ApEn = 0.18) was significantly higher than that in healthy elderly (i.e., mean ApEn = 0.13),  
312 indicating increased irregularities and randomness in their gait patterns and an indication of loss of gait  
313 control. Interestingly, mean MFC was also higher in falls-risk elderly, supporting the authors' hypothesis  
314 that increasing MFC height could be a strategy to minimize tripping, and therefore risk of falling. MFC

315 variability, as assessed by ApEn, could potentially be used as a diagnostic marker for early detection of falls  
316 risk in older adults.

317 Lately, [Cavanaugh et al.](#)<sup>53</sup> explored the natural ambulatory activity patterns of community-dwelling  
318 older adults. Using a step activity monitor, the ambulatory activity data (i.e., series of one-minute step  
319 counts) were collected continuously (24 hours per day) for two weeks. Each series of one-minute step  
320 counts contains a two-dimensional temporal structure: (1) a vertical structure composed of one-minute step  
321 count values of varying magnitude, and (2) a binary horizontal structure composed of minutes containing  
322 either some activity (step count > 0) or no activity (step count = 0). Fluctuations in the vertical and  
323 horizontal structures form a unique pattern that reflects the individual's ambulatory activity pattern.  
324 Participants were divided into three groups based on the mean number of steps per day: highly active (steps  
325  $\geq 10,000$ ), moderately active ( $5,000 \leq \text{steps} \leq 10,000$  steps), and inactive (steps < 5,000 steps). ApEn was  
326 one of the nonlinear measures used to examine the complexity of daily time series composed of one-minute  
327 step count values. Specifically, ApEn determined the probability that short sequences of consecutive one-  
328 minute step counts repeated, at least approximately, throughout the longer temporal sequence of 1,440  
329 daily one-minute intervals. The authors used a short sequence length of 2 and a criterion of similarity of 0.2  
330 times the standard deviation of individual time series for all participants. The results highlighted the  
331 unpredictability of minute-to-minute fluctuations in activity of highly active participants and the relative  
332 greater regularity in the activity patterns of less active participants. Specifically, highly active participants  
333 displayed greater amounts of uncertainty (i.e., mean ApEn = 0.50) in the vertical structure of the step count  
334 time series than either moderately active (i.e., mean ApEn = 0.40) or inactive participants (i.e., mean ApEn  
335 = 0.28). Given the fact that step count data demonstrated a deterministic pattern, greater uncertainty was  
336 interpreted as greater complexity. Therefore, the authors inferred that a higher level of activity might be  
337 associated with an enhanced ability to adapt walking behaviour to sudden changes in task demands or  
338 environmental conditions, an important feature of healthy aging. This study provided a field-based  
339 methodological approach that offers an "ongoing view" of walking, that is, an opportunity to study the  
340 manner in which an older adult interacts naturally with the customary environment, beyond the spotlight  
341 of the clinical and laboratory settings.

#### 342 4.2.2. Detrended Fluctuation Analysis

343 [Hausdorff et al.](#)<sup>2,8</sup> observed that the gait of healthy young adults exhibits long-range, self-similar  
344 (fractal) correlations. The authors collected stride time intervals during overground walking using force  
345 sensitive switches, and analyzed them using the Detrended Fluctuation Analysis. They found that the  
346 scaling exponent (i.e., a measure of the degree to which a stride interval at a given time scale is correlated  
347 with previous and subsequent stride intervals over different time scales) is  $\alpha = 0.76$  in self-paced conditions.  
348 Interestingly, the scaling exponent  $\alpha$  remained relatively constant ( $\alpha$  ranging from 0.84 to 1.10) in slow and  
349 fast paced conditions. Subsequent studies supported these findings, demonstrating that the fractal property  
350 of the fluctuations in the stride interval is also present during treadmill walking or running<sup>57-59</sup>. From a  
351 neurophysiological control viewpoint, it appears that the presence of long-term, dependence (or "memory"  
352 effect) in gait is intrinsic to the locomotor control system and exist for a wide range of gait velocities.  
353 Another study compared the stride interval fluctuations of healthy elderly (i.e., free of underlying disease)

354 vs. young adults<sup>9</sup>. The scaling exponent  $\alpha$  was significantly lower in the elderly compared to the young ( $\alpha =$   
355 0.68 vs. 0.87, respectively), indicating a loss of long-range correlations with aging. Although  $\alpha$  differed in  
356 the two age groups, the traditional measures (mean and coefficient of variation of stride time intervals)  
357 were not altered with age. Therefore, it appears that the DFA scaling exponent  $\alpha$  is a sensitive measure able  
358 to detect even subtle age-related changes in locomotor function.

359 In the effort to characterize the biological “clock” that controls locomotion, Hausdorff et al.<sup>8</sup> examined  
360 fluctuations in the stride interval during metronomically-paced walking. Healthy young adults walked in  
361 time with the metronome’s beat set to the subject’s natural stride time interval. The metronomic conditions  
362 breakdown the typical long-range correlations of the stride intervals typically found in self-paced walking,  
363 meaning that successive stride intervals became uncorrelated. The authors explained this breakdown by  
364 suggesting that supraspinal influences (i.e., locomotor pacesetter above the level of the spinal cord) could  
365 override the normally present long-range correlations generated peripherally. In other words, the  
366 intervention of attentional and intentional processes focused on external pacing would provoke a kind of  
367 “over-simplification” of the system, yielding the deterioration of long-range correlation in stride interval  
368 fluctuations. However, Delignière and Torre<sup>63</sup> recently re-examined Hausdorff et al.’s data and showed  
369 that in metronomic conditions stride intervals cannot be considered as uncorrelated, but rather, contained  
370 anti-persistent correlations ( $0.34 < \alpha < 0.41$ ). The authors concluded that the intrinsic complexity of the  
371 system is still at work in metronomic conditions, but expresses differently in overt performance. According  
372 to them, the presence of long-range dependencies in stride time intervals is determined by a central  
373 timekeeper possessing fractal properties. In metronomic conditions, an auto-regressive correction process  
374 would control the discrepancy between the periods produced by this timekeeper and those imposed by the  
375 metronome.

376 To gain insight into the basis of the presence of long-term dependence, Hausdorff et al.<sup>9</sup> investigated  
377 the effects of a neurodegenerative condition, the Huntington’s disease, on long-range correlations in stride  
378 time fluctuations. The rationale behind the study of patients with Huntington’s disease is that they are  
379 generally adults between 30-40 years old with impairment limited primarily to the central nervous system  
380 (i.e., free of other comorbidities and peripheral disease), thus providing a “contrast” to aging to better  
381 understand the mechanisms underlying the existence of stride-interval correlations. Most of the  
382 Huntington’s disease-related changes have been observed in the basal ganglia, with a loss of striatal  
383 projection neurons. Reduced stride-interval correlations were observed for the patients with Huntington’s  
384 disease ( $\alpha = 0.60$ ) compared with healthy controls ( $\alpha = 0.88$ ), indicating the apparition of an “unhealthy”,  
385 uncorrelated (or anti- persistent) dynamics. Besides, among the patients with Huntington’s disease,  $\alpha$  was  
386 inversely correlated with disease severity. The authors suggested that the striatal pathology (that leads to a  
387 decrease in fine motor control) might also impair the long-term dependence and fine control required for  
388 stride-interval correlations. Collectively, these results lay emphasis on the importance of the central nervous  
389 system in the generation of the fractal property of gait.

390 More recently, Hermann et al.<sup>64</sup> investigated whether the scaling exponent  $\alpha$  could be used as a  
391 predictor of falls in older adults with a higher-level gait disorder that is an altered gait that is not a result of  
392 lower extremity or peripheral dysfunction and cannot be attributed to well defined chronic disease (e.g.,

393 idiopathic “cautious” gait of the elderly<sup>65</sup>). Among these patients, all measures (of muscle function, balance,  
394 and gait, including gait speed and stride time variability) were similar in fallers and non-fallers (including  
395 fear of falling). Only the scaling exponent  $\alpha$  was significantly decreased in fallers (i.e.,  $\alpha = 0.75$  in fallers vs.  
396 0.88 in non-fallers), indicating that the walking pattern of the fallers was more random and spatio-  
397 temporally less organized. Changes in the temporal ordering of the stride interval pattern in fallers have  
398 been suggested to reflect changes in specific cognitive domains. Hausdorff et al.<sup>66</sup> demonstrated that, to a  
399 large degree, the cognitive profile of fallers is similar to that of patients with Parkinson’s disease (PD), with  
400 prominent deficits in executive function and attention. However, unlike PD patients, fallers were  
401 abnormally inconsistent in their response times when performing a Go/No-go response inhibition  
402 paradigm. Using sensitive neuroimaging techniques, Bellgrove et al.<sup>67</sup> found that those individuals with  
403 increased inconsistent response times activate inhibitory regions to a greater extent, perhaps reflecting a  
404 greater requirement for top-down executive control. Collectively, these findings suggested that fallers may  
405 have damage to specific neural networks, in particular those subserving executive function and attention.

## 406 5. Modeling gait complexity

407 Complexity in human gait has also been considered from a modelling standpoint in order to gain  
408 insights into the origins of the chaotic dynamics<sup>2,17,68-71</sup>. Indeed, even if studies well-established that chaos  
409 relates to flexibility in gait, generating stable and variable patterns, they did not bring information about the  
410 principles that govern such a chaotic aspect. Within this line of research, different efforts have then been  
411 made to identify quite simple models (also called templates<sup>72</sup>) able to reproduce chaos, and, more  
412 interesting, which can be used to investigate how chaos in gait can be controlled by the neural system.

413 One effort for exploring chaotic locomotion has been made using a passive dynamic double pendulum  
414 model that walks down a slightly sloped surface, where one leg is in contact with the ground and the other  
415 leg swings freely with the trajectory of the system’s center of mass<sup>15-17,69</sup> (Fig. 4A). Using the step time  
416 interval as an output of the model, the authors showed a cascade of period-doubling bifurcations as a  
417 function of the slope, starting with a period of one for the low slopes (i.e., same time interval for every step  
418 of locomotion) characterizing a periodic (limit-cycle) gait pattern and multiple periods for the high slopes  
419 (i.e., different time interval for the steps of locomotion) leading to a chaotic gait pattern (Fig. 4B). A state  
420 space examination was also conducted from the simulated step time interval data series and the largest  
421 Lyapunov exponents were found to be first null and later positive, confirming the successive bifurcations  
422 from a periodic to a strange (chaotic) attractor with the slope. Hence, despite its simplicity, the model  
423 produced chaotic walking patterns with no active control, meaning that chaos may actually underlie the  
424 normal dynamics of the neuromuscular system. Also, a major aim of the authors was to connect such  
425 complex locomotive dynamics with active neural control mechanisms to understand how the nervous  
426 system can take advantage and utilize the properties of the attractors generated by the model, and  
427 especially of the strange attractor. Using an artificial neural network (ANN) that modulates hip joint  
428 actuation (i.e., by setting the joint stiffness) during the leg swing, Kurz and Stergiou<sup>15,17</sup> showed the  
429 possibility to induce transitions between the period- $n$  gait patterns (i.e., any step time intervals) of the  
430 model. In particular, while the model would be unstable and fall down for highly slope values, the ANN

431 was capable of selecting a hip joint actuation that transitioned the locomotive system to a stable gait that  
432 was embedded in the chaotic attractor and prevented falls. Also, faced an unforeseen perturbation, the  
433 ANN was capable of selecting a hip joint actuation that rapidly transitioned the locomotive system to a  
434 stable gait, preventing falls again. Hence, such results strongly support that chaos provide flexibility in the  
435 neuromuscular system by providing a mechanism for transitioning to stable gait patterns that are embedded  
436 in the chaotic system (as required in the ever-changing walking environment) and that changes in the  
437 chaotic structure of gait pattern observed in the literature may be related to the neural control of the gait  
438 pattern.

439 *Please insert Fig. 5 here*

440 Another significant modelling effort of the human locomotion that governs the stride time interval  
441 series has been made using a family of stochastic network of neurons, or central pattern generators (CPG),  
442 capable of producing syncopated output<sup>2,68</sup>. Specifically, these models take the form of a random walk  
443 moving on a finite-size correlated chain of virtual firing nodes, each node generating an impulse of  
444 particular intensity that induce an output signal of particular frequency. Using such a network structure, the  
445 authors were capable of producing stride time interval time series with long term correlations as those  
446 observed normally in human walking (i.e.,  $0.5 < \alpha \leq 1$ ). West and Scafetta<sup>70</sup> and Scafetta et al.<sup>71</sup> have  
447 then proposed an extension of these models, called the super-CPG, in which the authors coupled a  
448 stochastic CPG to a Van der Pol oscillator. In others words, while the first models only aimed to reproduce  
449 the chaotic properties of gait using a schematic neural structure, this model is based on the assumption that  
450 human locomotion is regulated both by the nervous system (through the stochastic CPG) and the motor  
451 control system (through the oscillator). The model assumes that each cycle of the oscillator, which  
452 represents the lower limb, is initiated with a new virtual inner frequency produced by the stochastic CPG.  
453 However, the real stride-interval coincides with the actual period of each cycle of the Van der Pol oscillator,  
454 its period depending of the inner frequency coming from the stochastic CPG but also on the amplitude and  
455 the frequency of an external forcing function. Accordingly, the gait frequency and then the time stride  
456 interval are slightly different from the inner frequency induced by the neural firing activity. The authors  
457 then modulated the strength of the forcing function in order to force the frequency of the cycle as in under  
458 metronome-triggered gait conditions (i.e., conscious stresses). It was observed that the properties of the  
459 generated time series were similar to those observed from the experiments with an increase in randomness.  
460 As a consequence, these results seem to prove that the control of the chaotic gait structure would come  
461 from low and high nervous centres, including spinal neural networks (i.e., CPGs) and more “voluntary”  
462 nervous structures (i.e., the central nervous system).

## 463 **6. Conclusions**

464 In this review, most commonly used nonlinear tools for the exploration of gait complexity were  
465 described as well as their potential importance to provide insight into mechanisms underlying  
466 “pathological” conditions of human gait. Far from being a source of error, evidence supports the necessity  
467 of an optimal state of variability for health and functional movement. Healthy systems exhibit “organized”  
468 variability. In gait, disease (e.g., idiopathic fallers) or unhealthy (e.g., physical inactivity) states may  
469 manifest with increased or decreased complexity of lower extremities walking behaviour as it was found in

470 elderly fallers compared with healthy controls and in inactive older adults compared to those that are more  
471 active. Unhealthy state is also associated with a loss of self-similarity and long-range dependence. For  
472 instance, DFA, a measure of long-range persistence (dependence), was found to be decreased in fallers, and  
473 even more in patients with Huntington’s disease, with the apparition of an uncorrelated (or anti- persistent)  
474 dynamics. These findings are completely in line with earlier findings in human physiology, suggesting that  
475 the pathological state should be better conceptualized as a part of “dynamic reordering” rather than as  
476 manifestations of a disordering process<sup>73</sup>. The concepts of variability and complexity, and the nonlinear  
477 tools used to measure these concepts open new vistas for research in gait dysfunction of all types. Besides,  
478 the recent modelling effort of the human locomotion provided the groundwork to better understand how  
479 motor control strategies and the mechanical constructs of the locomotion system influence the chaotic  
480 properties (complexity) of the gait.

481

#### 482 **Acknowledgments**

483 This work is supported by the NIH (K25HD047194), the NIDRR (H133G040118 and  
484 H133G080023), the Nebraska Research Initiative, and the Department of Geriatrics of the University of  
485 Nebraska Medical Center.

486



487 **References**

- 488 1. Vaughan CL. Theories of bipedal walking: an odyssey. *J Biomech*, 2003, 36:513-523.
- 489 2. Hausdorff JM, Peng CK, Ladin Z, Wei JY, Goldberger AL. Is walking a random walk? Evidence for  
490 long-range correlations in the stride interval of human gait. *J Appl Physiol*, 1995, 78:349-358.
- 491 3. Dingwell JB, Cusumano JP. Nonlinear time series analysis of normal and pathological human walking.  
492 *Chaos*, 2000, 10: 848-863.
- 493 4. Stergiou N, Buzzi UH, Kurz MJ, Heidel J. (2004). Nonlinear Tools in Human Movement. In N.  
494 Stergiou (Ed.), *Innovative Analyses of Human Movement* Champaign, IL: Human Kinetics. 2004, pp.  
495 63-90.
- 496 5. Gleick J. *Chaos: making a new science*. New York: Viking Penguin.1987.
- 497 6. Glass L, Mackey MC. *From clocks to chaos: The rhythms of life*. Princeton, NJ: Princeton University  
498 Press. 1988.
- 499 7. Amato I. Chaos breaks out at NIH, but order may come of it. *Science*, 1992, 257:1763-1764.
- 500 8. Hausdorff JM, Purdon PL, Peng CK, Ladin Z, Wei JY, Goldberger AL. Fractal dynamics of human  
501 gait: Stability of long-range correlations in stride interval fluctuations. *J Appl Physiol*, 1996, 80:1448-  
502 1457.
- 503 9. Hausdorff JM, Mitchell SL, Firtion R, Peng CK, Cudkowicz ME, Wei JY, Goldberger AL. Altered  
504 fractal dynamics of gait: reduced stride-interval correlations with aging and Huntington's disease. *J*  
505 *Appl Physiol*, 1997, 82:262-269.
- 506 10. West BJ, Griffin L. Allometric control of human gait. *Fractals*, 1998, 6:101-108.
- 507 11. West BJ, Griffin L. Allometric control, inverse power laws and human gait. *Chaos Solitons Fractals*,  
508 1999, 10:1519-1527.
- 509 12. Dingwell JB, Cusumano JP, Sternad D, Cavanagh PR. Slower speeds in patients with diabetic  
510 neuropathy lead to improved local dynamic stability of continuous overground walking. *J Biomech*,  
511 2000, 33:1269-1277.
- 512 13. Dingwell JB, Marin LC. Kinematic variability and local dynamic stability of upper body motions  
513 when walking at different speeds. *J Biomech*, 2006, 39, 444-452.
- 514 14. Buzzi UH, Stergiou N, Kurz MJ, Hageman PA, Heidel J. Nonlinear dynamics indicates aging affects  
515 variability during gait. *Clin Biomech*, 2003, 18, 435-443.
- 516 15. Kurz MJ, Stergiou N. Hip actuations can be used to control bifurcations and chaos in a passive  
517 dynamic walking model. *J Biomech Eng- T ASME*, 2007, 129:216-222.
- 518 16. Kurz MJ, Stergiou N. Do horizontal propulsive forces influence the nonlinear structure of locomotion?  
519 *J Neuroeng Rehabil*, 2007, 15, 4:30.
- 520 17. Kurz MJ, Stergiou N. An artificial neural network that utilizes hip joint actuations to control  
521 bifurcations and chaos in a passive dynamic bipedal walking model. *Biol Cybern*, 2005, 93, 213-221.
- 522 18. Goldberger AL, Rigney DR, West BJ. Chaos and fractals in human physiology. *Sci Am*, 1990,  
523 262(2):42-49
- 524 19. Rabinovich MI, Abarbanel HDI. The role of chaos in neural systems. *Neuroscience*, 1998, 87:5-14.
- 525 20. Glass L. Synchronization and rhythmic processes in physiology. *Nature*, 2001, 410:277:284.

- 526 21. Peng CK, Mietus J, Hausdorff JM, Havlin S, Stanley HE, Goldberger AL. Long-range anticorrelations  
527 and non-Gaussian behavior of the heartbeat. *Phys Rev Lett*, 1993, 70:1343-1346.
- 528 22. Parati G, Saul JP, Di Rienzo M, Mancia G. Spectral analysis of blood pressure and heart rate  
529 variability in evaluating cardiovascular regulation. *Hypertension*, 1995, 25:1276-1286.
- 530 23. Lombardi F, Malliani A, Pagani M, Cerutti S. Heart rate variability and its sympatho-vagal  
531 modulation. *Cardiovasc Res*, 1996, 32:208-216.
- 532 24. Bigger JT Jr, Steinman RC, Rolnitzky LM, Fleiss JL, Albrecht P, Cohen RJ. Power law behavior of  
533 RR-interval variability in healthy middle-aged persons, patients with recent acute myocardial  
534 infarction, and patients with heart transplants. *Circulation*, 1996, 21:2142-2151.
- 535 25. Ivanov PC, Amaral LA, Goldberger AL, Havlin S, Rosenblum MG, Struzik ZR, Stanley HE.  
536 Multifractality in human heartbeat dynamics. *Nature*, 1999, 399:461-465.
- 537 26. Lombardi F. Chaos Theory, Heart Rate Variability, and Arrhythmic Mortality. *Circulation*,  
538 2000,101:8-10
- 539 27. Stergiou N, Harbourne RT, Cavanaugh JT. Optimal movement variability: A new theoretical  
540 perspective for neurologic physical therapy. *J Neurol Phys Ther*, 2006, 30, 120-129.
- 541 28. Goldberger AL, Amaral LA, Hausdorff JM, Ivanov PC, Peng CK, Stanley HE. Fractal dynamics in  
542 physiology: Alterations with disease and aging. *Proceedings of the National Academy of Sciences*  
543 U.S.A, 2002, 99(Suppl. 1):2466-2472.
- 544 29. Kantz H, Schreiber S. *Nonlinear time series analysis (2<sup>nd</sup> edition)*. Cambridge University Press,  
545 Cambridge, UK. 1997.
- 546 30. Strogatz SH. *Nonlinear Dynamics and Chaos: With Applications to Physics, Biology, Chemistry, and*  
547 *Engineering*. Addison Wesley, Reading, MA. 1994.
- 548 31. Gates DH, Dingwell, JB. Comparison of different state space definitions for local dynamic stability  
549 analyses. *J Biomech*, 2009; 42(9):1345-1349.
- 550 32. Ruelle D, Takens F. On the nature of turbulence. *Commun Math Phys*, 1971, 20,167-192.
- 551 33. Takens F. Detecting strange attractors in turbulence. In: Rand, D. and Young, L.S. (Eds.), *Dynamical*  
552 *systems and turbulence*, warwick 1980. Springer, Berlin. 1981, Vol. 898, pp. 366-381.
- 553 34. England, SA, Granata, KP. The influence of gait speed on local dynamic stability of walking. *Gait*  
554 *Posture* 2007, 25(2):172-178.
- 555 35. Bruijn, SM, van Dieen, JH, Meijer, OG, Beek PJ. Statistical precision and sensitivity of measures of  
556 dynamic gait stability. *J Neurosci Meth*, 2009, 178(2):327-333.
- 557 36. Dingwell J, Robb, R, Troy K, Grabiner M. Effects of an attention demanding task on dynamic stability  
558 during treadmill walking. *Journal of Neuroeng Rehabil*, 2008, 5(1), 12.
- 559 37. Jordan K, Challis JH, Cusumano JP, Newell KM. Stability and the time-dependent structure of gait  
560 variability in walking and running. *Hum Mov Sci*, 2009, 28(1):113-128.
- 561 38. Granata KP, England SA. Stability of dynamic trunk movement. *Spine*, 2006, 31(10):E271-E276.
- 562 39. Fraser AM, Swinney HL. Independent coordinates for strange attractors from mutual information,  
563 *Phys Rev A*, 1986, 33(2):1134-1140.
- 564 40. Kennel MB, Brown R, Abarbanel HDI. Determining embedding dimension for phase space-  
565 reconstruction using a geometrical construction, *Phys Rev A*, 1992, 45, 3403:3411.

- 566 41. Rosenstein MT, Collins JJ, De Luca CJ. A practical method for calculating largest Lyapunov  
567 exponents from small data sets. *Physica D*, 1993, 65, 117-134.
- 568 42. Grassberger P, Procaccia I. Measuring the strangeness of strange attractors. *Physica D*, 1983, 9, 189-  
569 208.
- 570 43. Theiler J. Spurious dimensions from correlation algorithms applied to limited time series data. *Phys*  
571 *Rev A*, 1986, 34(3), 2427-2432.
- 572 44. Grassberger P, Procaccia I. Characterization of strange attractors. *Phys Rev Lett*, 1983, 50:346-349.
- 573 45. Rapp PE. A guide to dynamical analysis. *Integr Psychol Behav*, 1994, 29:311-327.
- 574 46. Theiler J, Eubank S, Longtin A, Galdrikian B, Farmer JD. Testing for nonlinearity in time series: the  
575 method of surrogate data. *Physica D*, 1992, 58:77-94.
- 576 47. Miller JM, Stergiou N, Kurz MJ. An improved surrogate method for detecting the presence of chaos in  
577 gait. *J Biomech*, 2006, 39:2873-2876.
- 578 48. Theiler J, Rapp PE. Re-examination of the evidence for low-dimensional, nonlinear structure in the  
579 human electroencephalogram. *Electroen Clin Neuro*, 1996, 98:213-222.
- 580 49. Small M, Yu D, Harrison RG. Surrogate test for pseudoperiodic time series data. *Phys Rev Lett*, 2001,  
581 87(18):8101-188104.
- 582 50. Pincus SM. Approximate entropy as a measure of system complexity. *P Nat Acad Sci USA*, 1991,  
583 88:2297-2301.
- 584 51. Pincus SM, Goldberger AL. Physiological time-series analysis: what does regularity quantify? *The Am*  
585 *J Physiol*, 1994, 266, H1643:H1656.
- 586 52. Georgoulis AD, Moraiti C, Ristanis S, Stergiou N. A novel approach to measure variability in the  
587 anterior cruciate ligament deficient knee during walking: the use off the Approximate Entropy in  
588 Orthopaedics. *J Clin Monitor Comp*, 2006, 20:11-18.
- 589 53. Cavanaugh JT, Kochi N, Stergiou N. Nonlinear Analysis of Ambulatory Activity Patterns in  
590 Community-Dwelling Older Adults. *J Gerontol A Biol Sci Med Sci*, 2009, Oct 12
- 591 54. Peng CK, Havlin S, Stanley HE, Goldberger AL. Quantification of scaling exponents and crossover  
592 phenomena in nonstationary heartbeat time series. *Chaos*, 1995, 5:82-87.
- 593 55. Hausdorff JM. Gait dynamics, fractals and falls: Finding meaning in the stride-to-stride fluctuations of  
594 human walking. *Hum Mov Sci*, 2007, 26:555-589.
- 595 56. Decker LM, Rodríguez-Aranda C, Sara A. Myers CA, Jane F. Potter JF, Stergiou N. Dual-tasking that  
596 requires language perception, attention, and executive control processes have differential effects on  
597 stride width in young adults. *Exp Brain Res*, 2009, In press.
- 598 57. Frenkel-Toledo S, Giladi N, Peretz C, Herman T, Gruendlinger L, Hausdorff, JM. Treadmill walking  
599 as an external pacemaker to improve gait rhythm and stability in Parkinson's disease. *Mov Disord*,  
600 2005, 20:1109-1114.
- 601 58. Jordan K, Challis JH, Newell KM. (2006). Long range correlations in the stride interval of running.  
602 *Gait Posture*, 2006, 24:120-125.
- 603 59. Jordan K, Challis JH, Newell KM. Walking speed influences on gait cycle variability. *Gait Posture*,  
604 2007, 26:87-102.

- 605 60. Myers SA, Johanning JM, Stergiou N, Celis RI, Robinson L, Pipinos II. Gait variability is altered in  
606 patients with peripheral arterial disease. *J Vasc Surg*, 2009, 49(4):924-931.
- 607 61. Kurz M, Stergiou N. The aging neuromuscular system expresses less certainty for selecting joint  
608 kinematics during gait in humans. *Neurosci Lett*, 2003, 348:155-158.
- 609 62. Khandoker AH, Palaniswami M, Begg RK. A comparative study on approximate entropy measure  
610 and poincaré plot indexes of minimum foot clearance variability in the elderly during walking. *J*  
611 *Neuroeng Rehabil*, 2008 Feb 2;5:4.
- 612 63. Delignières D, Torre K. Fractal dynamics of human gait: a reassessment of the 1996 data of Hausdorff  
613 et al. *J Appl Physiol*, 2009, 106(4):1272-1279.
- 614 64. Herman T, Giladi N, Gurevich T, Hausdorff, JM. Gait instability and fractal dynamics of older adults  
615 with a "cautious" gait: why do certain older adults walk fearfully? *Gait Posture*, 2005, 21:178-185.
- 616 65. Nutt JG. Classification of gait and balance disorders. *Adv Neurol*. 2001, 87:135-141
- 617 66. Hausdorff JM, Doniger GM, Springer S, Yogev G, Giladi N, Simon ES. A common cognitive profile  
618 in elderly fallers and in patients with Parkinson's disease: The prominence of impaired executive  
619 function and attention. *Exp Aging Res*, 2006, 32, 411-429.
- 620 67. Bellgrove MA, Hester R, Garavan H. The functional neuroanatomical correlates of response  
621 variability: evidence from a response inhibition task. *Neuropsychologia*, 2004, 42(14):1910-1916.
- 622 68. Ashkenazy Y, Hausdorff JM, Ivanov P, Goldberger AL, Stanley AH. "A stochastic model of human  
623 gait dynamics". *Physica A*, 2002, 316, 662.
- 624 69. Kurz MJ, Stergiou N, Heidel J, Foster T: A template for the exploration of chaotic locomotive patterns.  
625 *Chaos, Solitons and Fractals*, 2005, 23:485-493.
- 626 70. West BJ, Scafetta N., "A nonlinear model for human gait," *Phys Rev E*, 2003, 67, 051917.
- 627 71. Scafetta N, Marchi D, West BJ. Understanding the complexity of human gait dynamics. *Chaos*, 2009,  
628 19(2):026108.
- 629 72. Full RJ, Koditschek DE. Templates and anchors: neuromechanical hypotheses of legged locomotion  
630 on land. *J Exp Biol*, 1999, 202, 3325.
- 631 73. Goldberger AL. Fractal variability versus pathologic periodicity: complexity loss and stereotypy in  
632 disease. *Perspectives in Biology and Medicine*. Publisher: Johns Hopkins University Press, 1997.

## Figures and captions

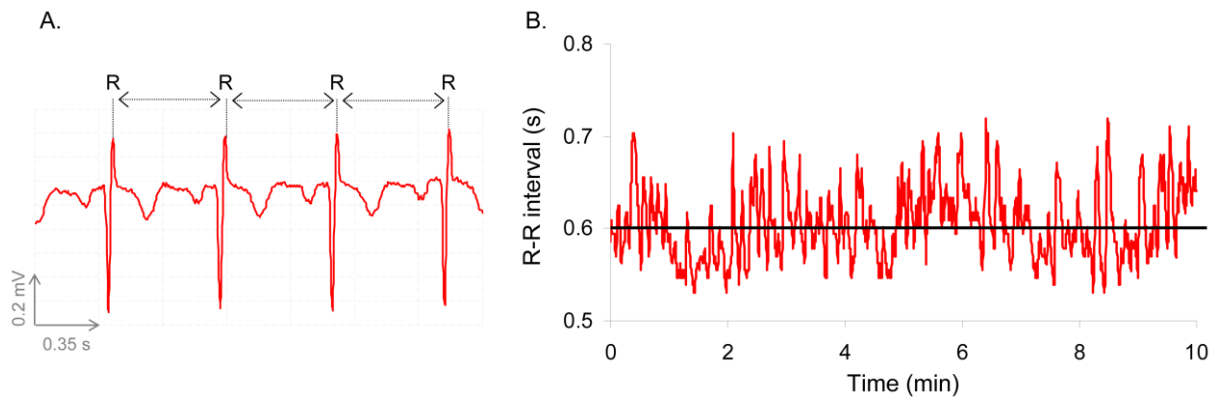


**Fig. 1.** Heart time series. **A.** An electrocardiogram (ECG) record, representing the electrical activity of the heart over time. The R-R interval represents the time duration between two consecutive R waves. **B.** R-R interval time series. Even though the interval is fairly constant, it fluctuates about its mean (solid line) in an apparently erratic manner. The data used for the traces A. and B. were obtained from the free web resources available on Physionet (<http://www.physionet.org>).

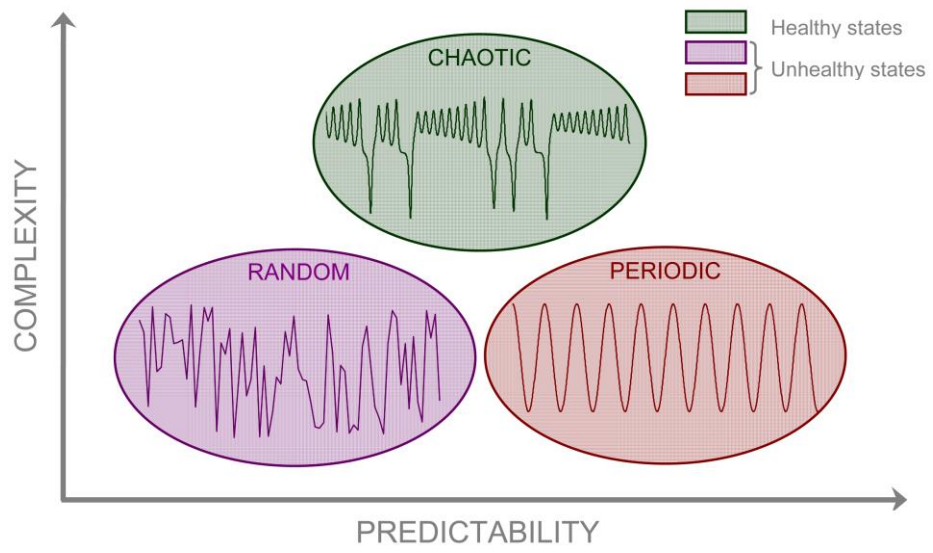


**Fig. 2.** Theoretical model of complexity as it relates to health. Adapted from [Stergiou et al.<sup>27</sup>](#)

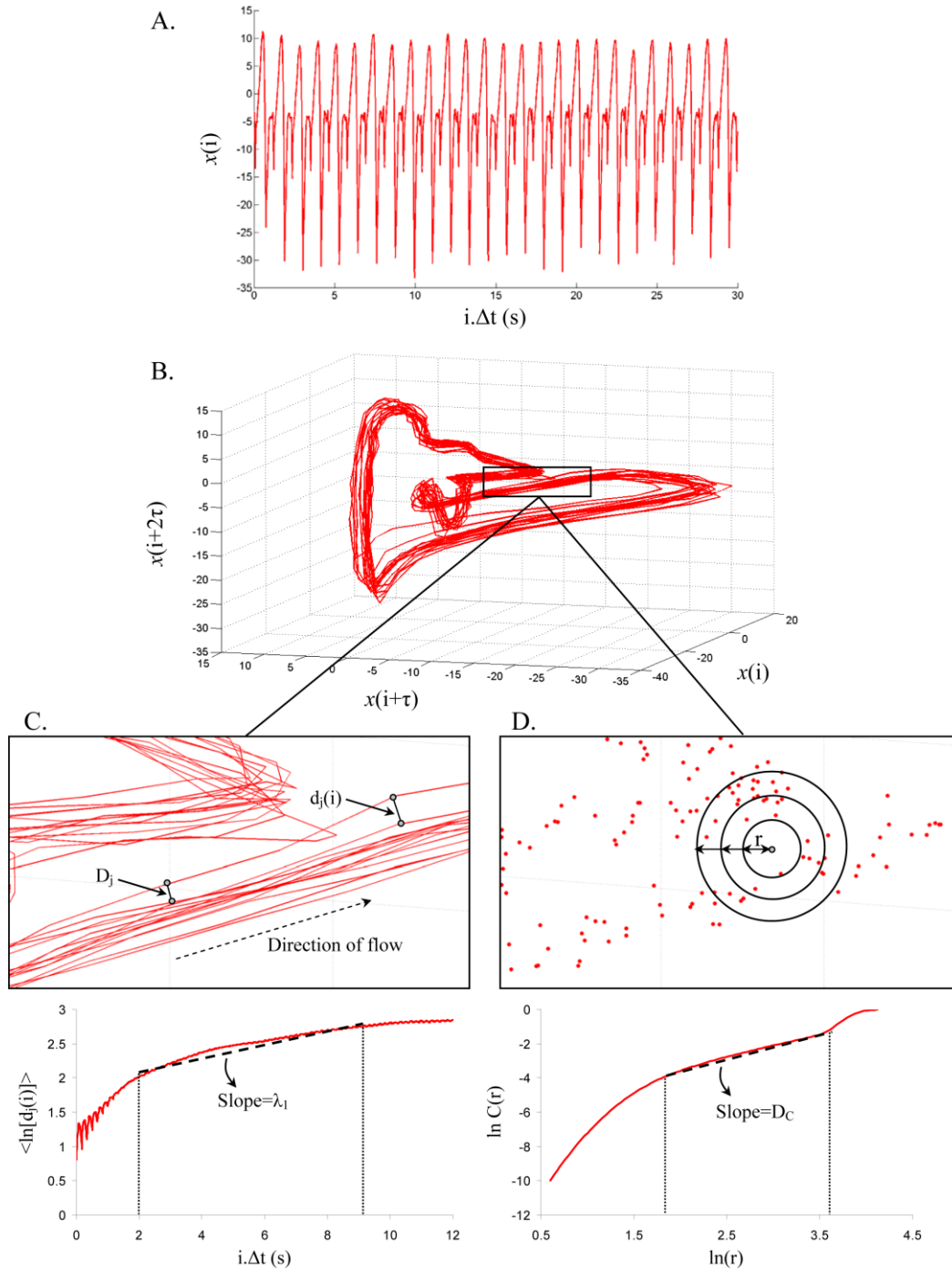


**Fig. 3.** State space analysis in human gait. **A.** A one-dimensional joint kinematics data set which is the hip angle over time in the saggittal direction. **B.** Reconstruction of the state space from the time series using the time delay method. For convenience, the state space is presented here with three embedding dimensions  $[x_i, x_{i+\tau}, x_{i+2\tau}]$ . Preferred states are visited in the space, corresponding to the attractor. Note that one complete orbit around the attractor constitutes one cycle of movement. **C.** Local section of the attractor where the divergence of neighbouring trajectories across  $i$  discrete time steps is measured by  $d_j(i)$ . The largest Lyapunov exponent  $\lambda_1$  is then calculated from the slope of the average logarithmic divergence of all pairs of neighbouring trajectories ( $\langle \ln[d_j(i)] \rangle$ ) versus  $i \cdot \Delta t$  s. **D.** Evaluation of the way in which the number of points within a sphere of radius  $r$  centred on the attractor scales with  $r$ . As the number of points,  $C(r)$ , increases as a power of  $r$ , the correlation dimension  $D_C$  is then calculated from the slope of the  $\ln/\ln$  plot of  $C(r)$  vs.  $r$ . The hip kinematics data were obtained from resources of the Nebraska Biomechanics Core Facility (University of Nebraska at Omaha).

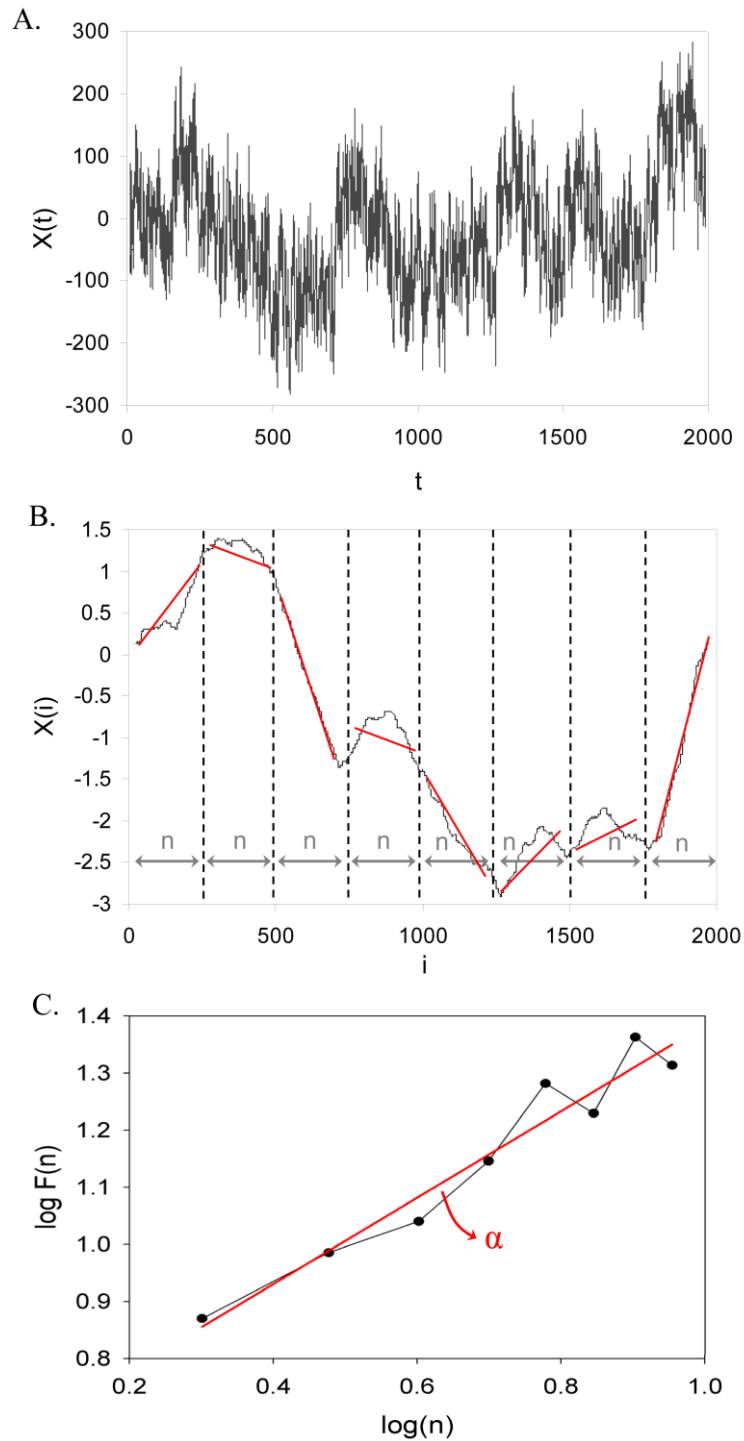


**Fig. 4.** Illustration of the detrended fluctuation analysis (DFA). **A.** The original time series. **B.** The original times series is integrated and divided into non-overlapping intervals of length  $n$ . In each interval, a least squares line is fit to the data and the series is locally detrended by subtracting the theoretical values given by the regression. The characteristic size of fluctuation  $F(n)$  for the integrated and detrended series is then obtained. **C.** Once the previous computation is repeated over all possible interval lengths, a power law between  $F(n)$  and  $n$  is expected. The scaling exponent  $\alpha$  is then expressed as the slope of a double logarithmic plot of  $F(n)$  as a function of  $n$ .



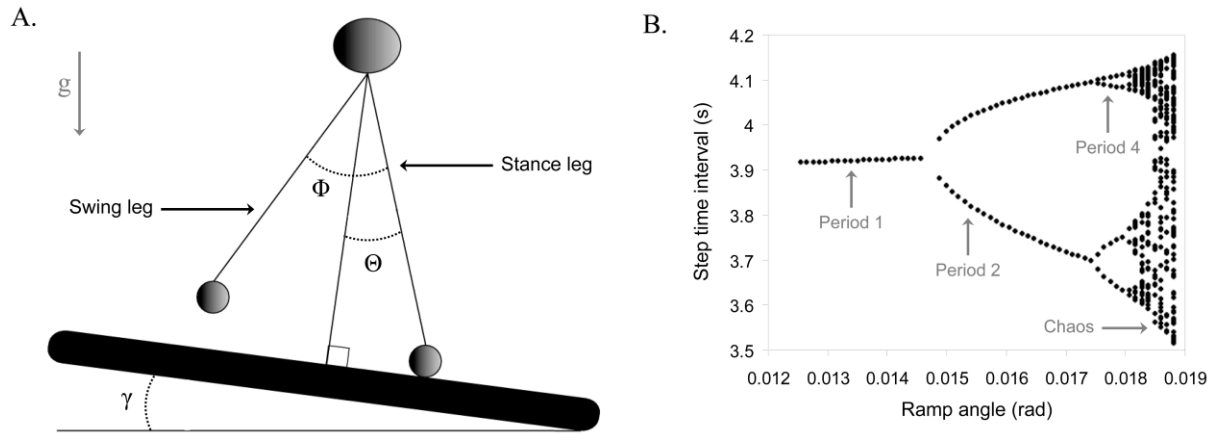


**Fig. 5. A.** Passive dynamic walking model that has a chaotic gait pattern. **B.** Bifurcation diagram of the gait patterns generated by the model as a function of the slope. The period is similar to the number of different step time intervals chosen by the walking model during a steady state gait. For example, period-1 means that the model adopt one step time interval during the gait and then a periodic pattern, period-2 that the model alternates between two different step time intervals revealing a quasi-periodic pattern, and so on until chaotic patterns.